Available online at www.sciencedirect.com
SCIENCE DIRECT®
Journal of Chromatography A, 1069 (2005) 53–64
JOURNAL OF CHROMATOGRAPHY A
www.elsevier.com/locate/chroma

Evaluating and monitoring the packing behavior of process-scale chromatography columns

Mark A. Teeters, Igor Quiñones-García *

Biotechnology Development, Schering-Plough Research Institute, 1011 Morris Avenue, U2-1500, Union, NJ 07083-7120, USA

Abstract

The packing characteristics of process-scale chromatography columns were evaluated using the responses to conductivity-based pulse and step inputs derived from tracer experiments and in-process transitions (i.e. column equilibration and regeneration steps). Characteristics of the measured residence time distributions (RTDs) were quantified by statistical moments and using the equations derived from the Gaussian model. The first and second moments calculated from in-process step transitions for multiple runs were in good agreement with those moments calculated from the pulse-input experiments conducted immediately after column packing. This indicates that most of the time the bed behavior at the time of packing is consistent with that at the time of operation. Due to the significant resistance to protein mass transfer inside the particles, estimated plate heights for protein solutes are expected to be much greater than those observed from the experiments using salt-based tracers. Thus, the column efficiency derived from salt-based experiments can be a useful measure of packing consistency rather than a significant parameter influencing the outcome of protein separations.

Keywords: Packing behavior; Process-scale chromatography columns; Column efficiency; Plate number; Residence time distribution; Statistical moments; Height equivalent of a theoretical plate

1. Introduction

Chromatography is widely used in the commercial production of therapeutic proteins, and as the process is scaled-up from the bench top to the pilot and production plants, it is important to maintain the performance of each chromatography step. Typical scale-up procedures entail keeping a constant linear velocity and bed height, so processing larger amounts of feed requires an increased column diameter. The use of large-diameter columns introduces challenges associated with achieving reproducible packing procedures and packing efficiencies which are consistent across different scales [1–3]. Contrary to the significant volume of available data regarding the efficiency of analytical-scale chromatography columns [4,5], there is a dearth of efficiency data for process-scale chromatography columns [6–11].

At the manufacturing scale, it is also important to maintain consistent packing characteristics for different beds used in multiple runs. It follows that monitoring packing characteristics of chromatography columns and understanding how they affect the step performance is critical in making decisions regarding the acceptance for use in manufacturing of an individual packed column [12]. Most often, freshly packed chromatography columns are evaluated by injecting a small pulse of a low molecular weight inert tracer (NaCl, acetone) into the top of the column and evaluating certain parameters from the effluent response. Acceptance or rejection of the packing considers whether some of these parameters fall within predefined ranges [12]. Accordingly, most of the published data for process-scale columns have been derived from pulse-input experiments [6–9,11]. Recent studies report column efficiencies approaching theoretical limits using pack-in-place columns fitted with multifunctional nozzle valves that operate in conjunction with an automated slurry packing system [6,7,9]. These systems provide a contained packing method that does not require column disassembly and re-assembly. The slurry is pumped into the column where the position of the flow distributor has been preset to a fixed bed height. The packing is complete when the pressure drop

* Corresponding author. Tel.: +1 908 820 6114; fax: +1 908 820 6112.
E-mail address: igor.quinones-garcia@spcorp.com
(I. Quiñones-García).

0021-9673/$ – see front matter © 2005 Elsevier B.V. All rights reserved.
doi:10.1016/j.chroma.2005.02.051

across the bed reaches a predefined maximum value and the slurry transfer pump stops.

In addition to utilizing the effluent response to a pulse-input, the column may be equivalently characterized from the response to a step input. This type of response may be observed, for example, after a conductivity step change during column equilibration or regeneration. There seems to be a smaller number of reports for process-scale columns dealing with characteristics derived from step inputs [10,13]. Larson et al. [10] recently investigated the utility of in-process step transitions for monitoring column performance by calculating an overall integrity value that proved effective in identifying problems that occurred after several runs.

During the purification of proteins derived from animal cell cultures, certain parameters characterizing the column responses to both pulse and step inputs might be very useful in order to assess the ability of a packed bed to deliver consistent viral clearance after multiple uses. It has been reported [14,15] that some parameters associated with the efficiency of the packed bed change simultaneously with the change of its virus removal capacity. Thus, in principle, certain RTD characteristics could be monitored as surrogates for virus clearance.

A number of different methods are available for evaluating the characteristics of the RTD, and the calculated packing efficiencies may vary greatly depending on which method is used [16,17]. The use of statistical moments has been recognized for a long time as one of the most accurate methods that can be applied to evaluate the RTD characteristics of chromatography columns [18–20]. Note that some of the published efficiency data for process-scale columns have been derived assuming a Gaussian peak profile [6,9] while other reports use the method of moments [7,10,13].

In this paper, we assess means of characterizing process-scale chromatography columns and tracking bed behavior over multiple uses. First investigated are different methods and approximations used to characterize packed bed RTDs, and the advantages and limitations associated with each method. Second, using both pulse-response data obtained immediately after column packing and step-response data obtained from manufacturing runs, we examine the consistency of the RTD properties obtained at different stages during the bed lifetime. This analysis allows insight into the stability of individual packed columns and indicates whether the packed bed characteristics are maintained throughout the operation. Finally, we investigate to which extent the RTD characteristics derived from salt-based tracer experiments can have a significant influence on the outcome of protein separations.

2. Methods

2.1. Media, columns and, systems

Sepharose Fast Flow sorbents (45–165 μm) were obtained from Amersham Biosciences (Uppsala, Sweden) and Fractogel EMD sorbents (40–90 μm) were obtained from Merck KGaA (Darmstadt, Germany). Process-scale chromatography columns (40–63 cm I.D.) and associated pack-in-place automated skids were obtained from either Amersham Biosciences or Millipore (Stonehouse, UK). Process-scale chromatography systems with UNICORN control software were obtained from Amersham Biosciences and used to obtain the chromatography traces.

2.2. Experimental procedures

Similar procedures to others reported for pack-in-place methods were also employed in this study [6–8]. Packed bed heights ranged from 21 to 29 cm. The linear velocity used to generate the RTDs ranged from 60 to 120 cm/h. All procedures were carried out in the cold room (2–8 °C).

Effluent conductivity responses to both pulse and step inputs of non-adsorbing salt tracers were obtained from packing evaluation tests and from in-process chromatography data. The conductivity measurements were between 1.0 and 160 mS/cm. For the pulse-input evaluation of freshly packed columns, the injected pulse of NaCl solution was approximately equal to 2% of the column volume. Before injecting the tracer, the columns were equilibrated with a NaCl solution of a lower concentration than the sample of the tracer in order to suppress NaCl retention.

The extra-column contribution to band broadening was found to be a small fraction of the overall peak dispersion. Representative data from multiple runs carried out in this study indicate that the extra-column dispersion is typically around 5% and never more than 10% of the overall dispersion for salt tracers. Note that the extra-column dispersion may vary from system to system (depending on the characteristics of the flow path) and even from run to run (depending on the volume of liquid held in the bubble trap during a particular run). Moreover, the pack-to-pack reproducibility of the column efficiency obtained from the operation of pack-in-place systems such as those used in this study has been reported to be around 6–7% [7]. Thus, the extra-column dispersion found in our experiments is of similar magnitude as the differences in efficiency that can be found from pack to pack. Finally, the extra-column dispersion has been reported to be an order of magnitude smaller than the dispersion originated in the column headers [7]. Accordingly, the results presented in this study should be representative of the contributions to dispersion from the packed column.

The linearity between the conductivity signal and the salt concentration was also verified for the data analyzed in this study. In order to conduct RTD analysis it is important to ensure that the signal measured (conductivity, optical density) is not affected by non-linear effects typically present at high concentrations of the tracer.

For the case of those responses to step inputs, it was necessary to find conductivity transitions that were the result of the step-input migrating through the column without any significant contribution from concurrent pH changes and/or

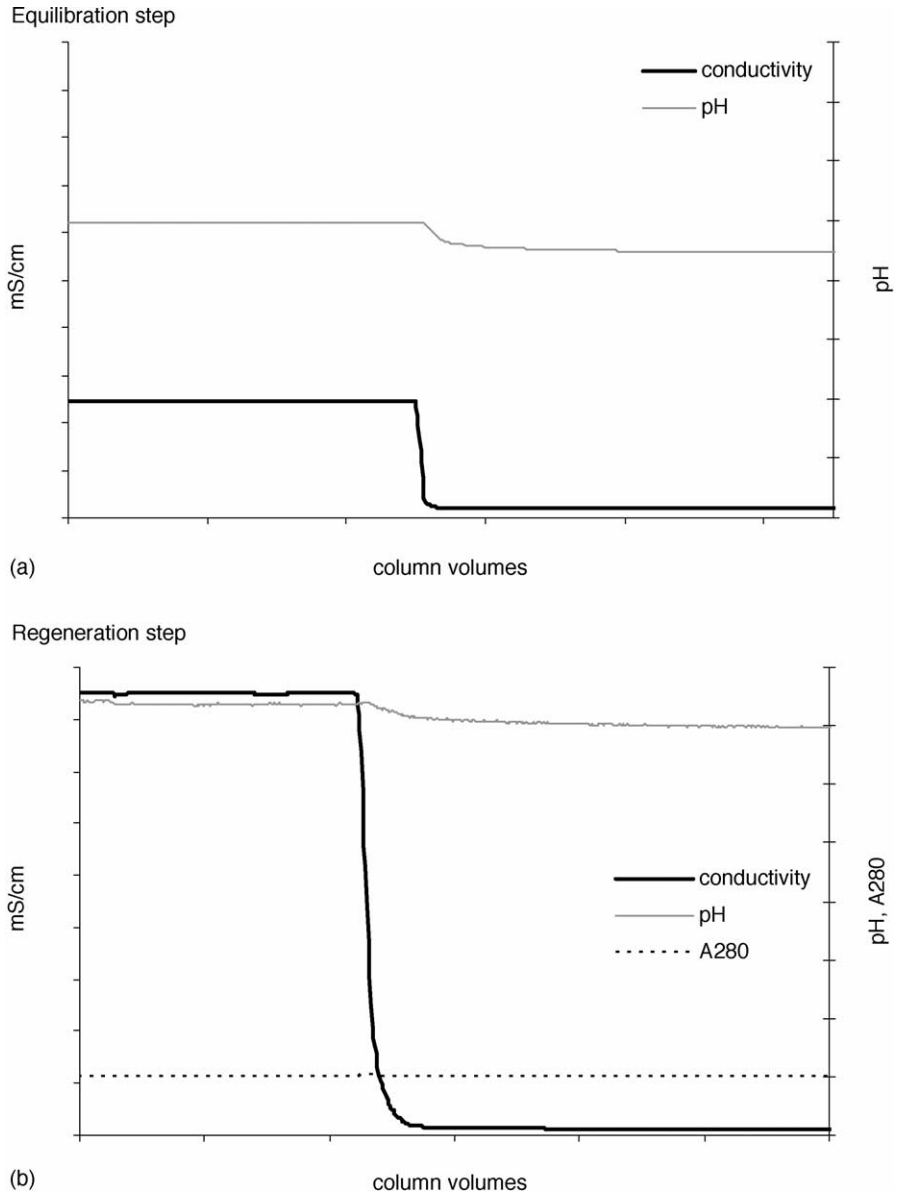

Fig. 1. Conductivity, pH, and A280 profiles for (a) equilibration and (b) regeneration steps associated with a specific purification process.

elution of bound species (proteins, etc.). This is an important requirement since RTD analysis is based on the use of an inert tracer. Fig. 1 provides examples of conductivity transitions from equilibration and regeneration steps that were found to be useful for RTD analysis.

2.3. Data analysis

Data files were opened using Unicorn 4.11 software (Amersham Biosciences, Piscataway, NJ, USA) and conductivity–volume data were exported for data analysis to either Excel 2002 (Microsoft, Redmond, WA, USA) or MATLAB Release 13 (MathWorks, Natick, MA, USA). Similar values of the RTD characteristics were calculated by either software package. The value of the elution volume at which either the pulse or the step input was introduced to the column was subtracted from the recorded volume data set in order to define the start of the vector containing the column response relevant to the analysis. The recorded conductivity vector was also adjusted by retaining for further analysis only those conductivity values that were associated with the adjusted volume vector.

2.3.1. Pulse-based RTDs

A baseline was established for the conductivity vector by subtracting the minimum recorded conductivity value from the entire conductivity data set. After this subtraction, the baseline noise was further filtered by assigning a value of zero to those conductivity values that were less than one percent of the conductivity value at the peak maximum. This

manipulation of the data was sufficient in order to minimize the noise from the analyzed data sets and maintain the dispersion of the RTD at the base of the peak.

2.3.2. RTD characteristics

The packing behavior of each column was characterized by moment-based estimations of the mean residence volume, variance, and skewness of each RTD, as outlined in the equations of Table 1 [18–20]. These column characteristics were determined by numerical integration of all RTD data. The values of the mean residence volume and variance were also estimated by approximating the RTD via the Gaussian model (see Table 1) and were compared to the respective moment-based estimations for all packed columns. In addition, asymmetry (A) at 10% of the peak maximum [12] was determined for each RTD and compared to the peak skewness. The position of the peak maximum, peak width at half height, and asymmetry were estimated using the UNICORN software.

2.4. Plate height definitions and correlations

Column efficiencies were estimated through the plate number, N, using

$$N_i = \frac{V_i^2}{\sigma_i^2} \tag{10}$$

where the subscript "i" refers to the solute. The reduced height equivalent of a theoretical plate, h, was determined using

$$h_i = \frac{L}{d_\mathrm{p} N_i} \tag{11}$$

where L represents the bed height and d_p is the particle diameter. While the plate number for the continuous plate model of chromatography is only truly defined for a Gaussian distribution (for $\sim N > 100$), as stated before, most real peaks are non-Gaussian and plate numbers are used as the most common measure of column efficiency by extending the use of Eq. (11) to all observed distributions [4].

All conductivity-based column efficiencies measured were derived from experiments where salt-based solutes were used as tracers. Because the actual separation of interest involves protein solutes, a predictive model describing the variation of plate height with solute size is necessary in order to gain further insight into the behavior of the systems being studied. Contributions to the overall reduced plate height (h_{i_overall}) of a packing include (i) molecular axial dispersion (h_{i_AD}), (ii) boundary-layer mass transfer (h_{i_BLMT}), (iii) intraparticle diffusion (h_{i_ID}), (iv) adsorption and desorption kinetics ($h_{i\_\mathrm{ADS/DES}}$), and (v) macroscopic dispersion (h_{i_MACRO}). With each individual contribution being additive, the overall reduced plate height may be expressed by [21]

$$h_{i\_\mathrm{overall}} = h_{i\_\mathrm{MACRO}} + h_{i\_\mathrm{AD}} + h_{i\_\mathrm{BLMT}} + h_{i\_\mathrm{ID}} + h_{i\_\mathrm{ADS/DES}} \tag{12}$$

where the value of the overall reduced plate height is a function of the nature of solute "i" (i.e. salt or protein), the mobile phase velocity, and the properties of the column and the packing media. The boundary-layer mass transfer and intraparticle diffusion terms may be estimated using the following equations [21]

$$h_{i\_\mathrm{BLMT}} = \frac{(1-x)^2}{3(1-\varepsilon_\mathrm{b})} \times ReSc_i \times \left(\frac{1}{Nu_i}\right) \tag{13}$$

Table 1
Different estimations of RTD characteristics

	Moment-based	Gaussian-based
RTD	Pulses[a]: $E(V) = \frac{c(V)}{\int_0^\infty c(V)\,\mathrm{d}V}$ (1)	$E(V) = \frac{1}{(2\pi\sigma^2_{\mathrm{Gaussian}})^{1/2}} \mathrm{e}^{-(V-V_{\mathrm{peak}})^2/2\sigma^2_{\mathrm{Gaussian}}}$ (8)
	Steps: $E(V) = \frac{\mathrm{d}F(V)}{\mathrm{d}V}$ (2)	
	where the age function is[b] $F(V) = \frac{c(V)-c_{\mathrm{initial}}}{c_{\mathrm{final}}-c_{\mathrm{initial}}}$ (3)	
Mean residence volume	$V_{\mathrm{mean}} = \int_0^\infty VE(V)\,\mathrm{d}V$ (4)	V_{peak}
Variance[c]	$\sigma^2_{\mathrm{moment}} = \int_0^\infty (V - V_{\mathrm{mean}})^2 E(V)\,\mathrm{d}V$ (5)	$\sigma^2_{\mathrm{Gaussian}} = \frac{W^2_{1/2}}{5.54}$ (9)
Asymmetry	–	1
Skewness	$s = \frac{\gamma^3}{(\sigma^2_{\mathrm{moment}})^{3/2}}$ (6)	0
	where $\gamma^3 = \int_0^\infty (V - V_{\mathrm{mean}})^3 E(V)\,\mathrm{d}V$ (7)	

[a] c is the conductivity and V is the elution volume. All integration was done using the trapezoidal rule.

[b] c_{initial} is the minimum (or maximum) conductivity value prior to the step change in conductivity and c_{final} is the maximum (or minimum) value after the step change. All differentiation was done numerically using a suitable smoothing technique (second-degree least squares with five points [19]). For a step change from high to low conductivity conditions, the absolute value of the derivative was taken in order to obtain positive values of the RTD.

[c] $W_{1/2}$ is the peak width at half height.

$$h_{i\_ID} = \frac{(1-x)^2}{3(1-\varepsilon_b)} \times ReSc_i \times \left(\frac{m}{10}\right) \quad (14)$$

Details of the model are provided by Athalye et al. [21] and definition of the terms may be found in the Nomenclature section. Because $h_{i\_ADS/DES}$ is generally small compared to other mass transfer contributions for the ion-exchange chromatography of proteins [3,19,22], this term was dropped from Eq. (12).

On the other hand, h_{i_MACRO} and h_{i_AD} are fairly insensitive to the solute diffusion coefficient [23]. Thus, the axial dispersion and macroscopic contributions to the reduced plate height can be assumed to be the same for a protein and for a low molecular weight, salt-based solute. Therefore, it follows that the contribution to the reduced plate height from both the axial and macroscopic band broadening can be calculated for any solute (either salt or protein) from (i) the knowledge of the overall reduced plate height for a salt-based solute determined from the experimental RTD data ($h_{salt\_overall}$) and (ii) the estimated values of the reduced plate height contributions due to film mass transfer (h_{salt_BLMT}) and intraparticle diffusion (h_{salt_ID}) for a salt-based solute, thus

$$\begin{aligned}(h_{protein\_AD} + h_{protein\_MACRO}) &= (h_{salt\_AD} + h_{salt\_MACRO}) \\ &= (h_{salt\_overall}) - (h_{salt\_BLMT} + h_{salt\_ID})\end{aligned} \quad (15)$$

The overall reduced plate heights for protein solutes can then be determined via Eq. (12) by adding the diffusional contributions estimated by Eqs. (13) and (14) to those approximated with Eq. (15).

3. Results and discussion

3.1. Evaluation of pulse-input RTDs

The comparison of RTD characteristics presented below for multiple packs of a representative column is based on (i) moment calculations and (ii) estimates based on the assumption of a Gaussian peak profile. While the data is only presented for a particular column, similar behavior was observed for all packed columns studied.

Depicted in Fig. 2 are the mean column volumes estimated using both the peak maximum location and the first moment of the pulse-input response. The location of the RTD peak maximum (V_{peak}) is only equal to the actual hold-up volume of the bed for a symmetrical peak, whereas the volume estimated by the first moment (V_{mean}) is independent of the peak shape. For the data presented in Fig. 2, V_{peak} is always smaller than V_{mean}, which is always the case for tailing peaks. *Pack*05 in Fig. 2 shows the largest discrepancy between the two estimates. If, in this case, V_{peak} was interpreted as the actual hold-up volume of the packed bed, it might be inferred that the position of the top column header needs adjustment in order to achieve the desired volume. Looking at V_{mean}, however, it becomes clear that the hold-up volume of *Pack*05 is consistent with other packs and that there is no need to change

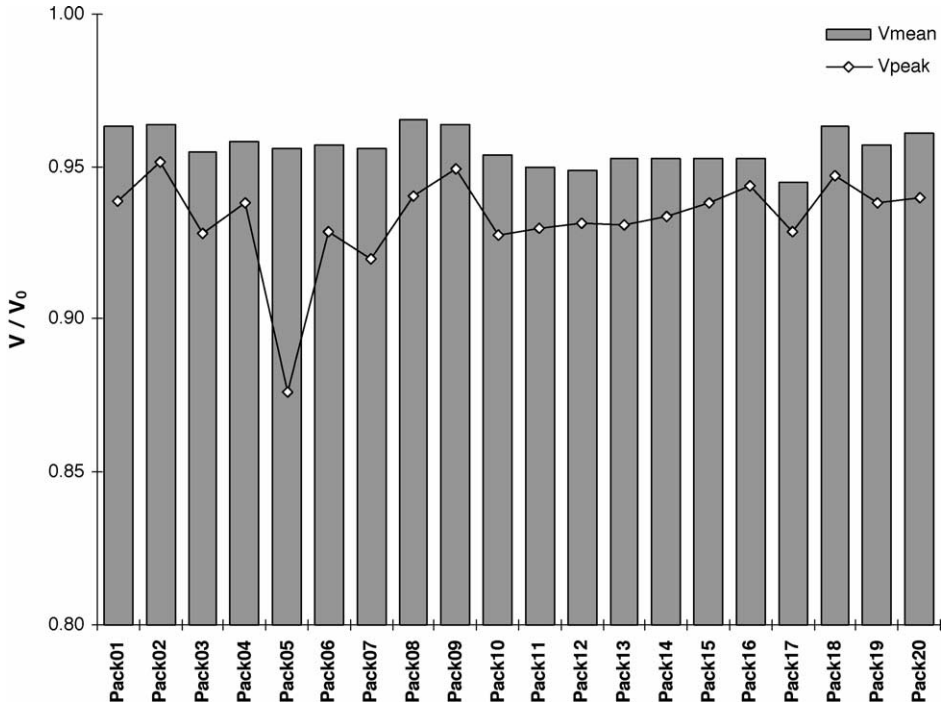

Fig. 2. Hold-up volume estimations for multiple packs of a representative process-scale chromatography column (63 cm internal diameter). The volumes were estimated from pulse-input RTDs using moments (Eq. (4)) and the position of the effluent peak maximum.

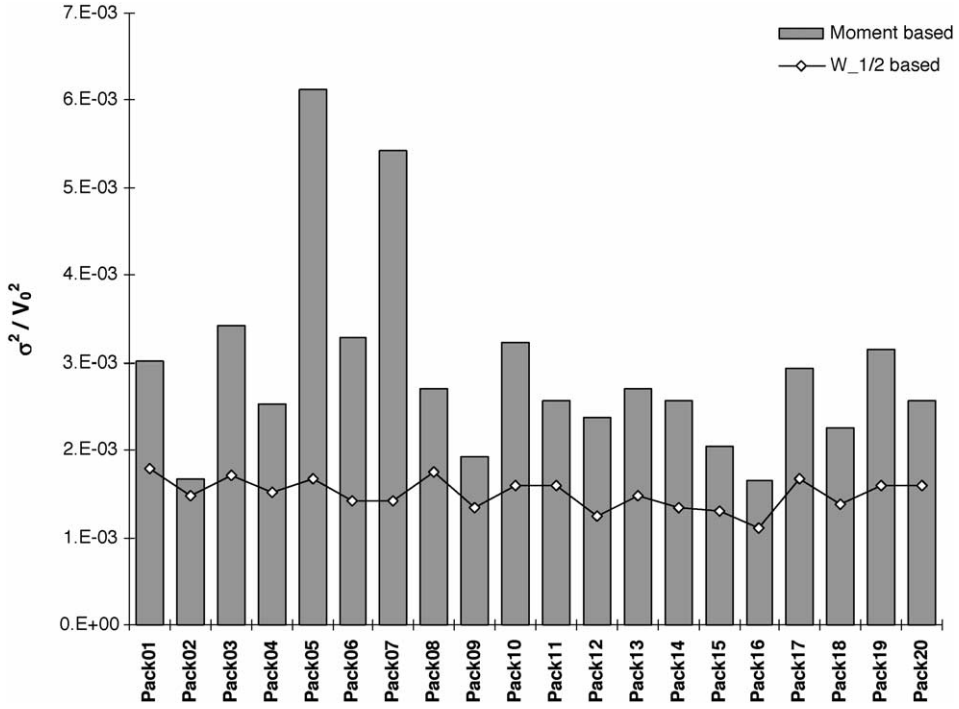

Fig. 3. RTD variance estimations for multiple packs of a representative process-scale chromatography column. Variances were estimated using moments (Eq. (5)) and the $W_{1/2}$ values (Eq. (9)).

the position of the flow distributor. This example shows that moment-based estimations of the column hold-up volume are more reliable than the estimate derived from the Gaussian model.

The variances estimated using (i) the peak width at half-height ($W_{1/2}$) via Eq. (9) derived from the Gaussian model and (ii) the second central moment via Eq. (5) are plotted in Fig. 3 for the same representative packs. The moment-based variances (σ^2_{moment}) are greater than the $W_{1/2}$-based variances ($\sigma^2_{\text{Gaussian}}$) since the former account for the dispersion over the entire RTD and are particularly sensitive to tailing in the vicinity of the baseline while the latter are based on only two points of the entire RTD and are, therefore, less sensitive to the dispersion present at the base of the peak.

Different measures of asymmetry are presented in Fig. 4 for the representative packs. Both the asymmetry at 10% of the peak maximum and the skewness defined in Eq. (6) indicate tailing RTDs for all columns evaluated. While both parameters correctly captured the type of asymmetry, there is not a strong correlation between the two sets of data presented in Fig. 4. There are two reasons that can contribute to the lack of a strong correlation. First, the moment-based calculation includes all points of the distribution and can offer increased sensitivity to tailing, especially to that occurring below 10% of the peak maximum. Second, the estimation error and the uncertainty associated with the noise of the RTD data increases when calculating higher order moments, such as the third central moment [1].

In Fig. 5, the third central moment (γ^3) is plotted against the second central moment (σ^2_{moment}). Over the range of the data observed for all large-scale columns investigated, the relationship between the two moments is roughly linear. This empirical correlation suggests that, in our case, the trend followed by the values of the third moment adds little additional insight into the characterization of the evaluated packed beds.

Finally, reduced plate height values for salt-based solutes were calculated using Eq. (11). The resulting moment-based estimates (using $L\sigma^2_{\text{moment}}/d_p V^2_{\text{mean}}$) and Gaussian-based estimates (using $LW^2_{1/2}/5.54 d_p V^2_{\text{peak}}$) are plotted in Fig. 6. The results of the reduced plate heights presented in Fig. 6 are in the range of 4–8 on the basis of the Gaussian model and 6–23 on the basis of the moment calculations, with most of the values calculated via moments in the range of 6–13. These results are in good agreement with recently published results [8,11]. As previously reported [16–17], these estimates of efficiency are largely dependent on the applied method of calculation, with moment-based estimates being greater than Gaussian-based estimates as a result of the larger values of the variance estimated via the statistical moments [18]. Notably, higher efficiencies have been reported recently for process-scale columns when the Gaussian model is employed [6,9] while lower efficiencies are reported when the method of moments is used [10].

Further examination of Fig. 6 reveals that the moment-based analysis is capable of detecting significant dispersion associated with peak tailing at the base of the peak while the Gaussian-based calculation is not. Take for example the cases of Pack05 and Pack07. Note that for these two packs the values of the reduced plate height calculated via moments are

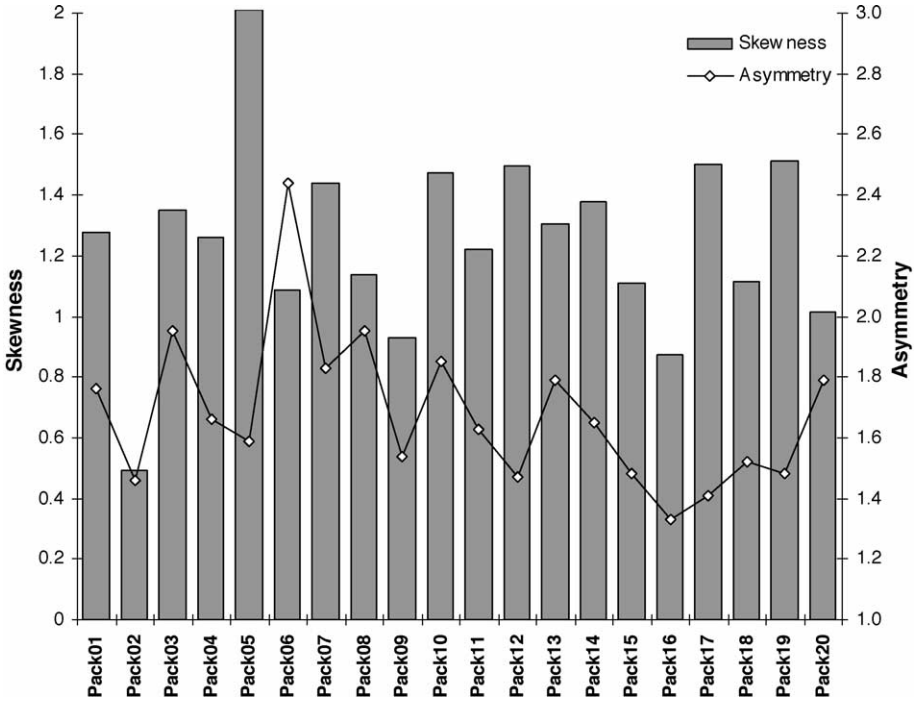

Fig. 4. RTD skewness and asymmetry estimations for multiple packs of a representative process-scale chromatography column. The skewness was evaluated using moments (Eq. (7)) and the asymmetry was evaluated at 10% of the peak maximum.

significantly higher than the efficiency values calculated on the basis of the Gaussian model. Moreover, note that the efficiency values calculated on the basis of the Gaussian model for these two packs follow the same trend as the rest of the data presented in Fig. 6. Thus, as a result of its low sensitivity to tailing close to the baseline, the Gaussian-based method fails to detect packed beds exhibiting unusually high dispersion, as noted elsewhere [10].

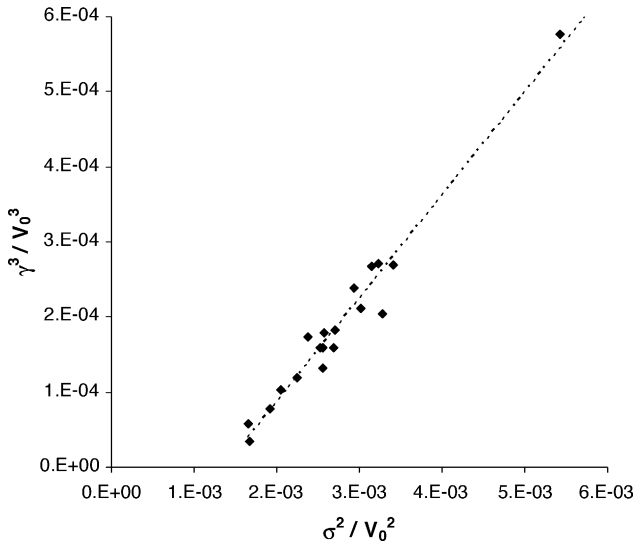

Fig. 5. The third central moment plotted against the second central moment for the column data presented in Figs. 3 and 4.

3.2. Evaluation of step input RTDs

The first and second central moments calculated from the RTDs obtained via the analysis of the step input transitions were compared to those moments calculated from the RTDs obtained via the analysis of the pulse-inputs for the same packed bed. In Fig. 7, the first moments, or mean residence volumes, calculated from a chosen equilibration step are plotted against the mean residence volumes calculated from the initial pulse-input evaluation. A similar analysis is presented in Fig. 8 for the second moments, or variances. Overall, there is good agreement between the moments calculated from the initial pulses and the subsequent in-process step transitions, thus indicating a stable packing behavior over multiple column uses. Only a few transitions (less than five percent) produced values of the moments markedly different from those originated by the initial salt pulse. Thus, monitoring stepwise, in-process transitions is a useful tool in order to determine if the bed behavior at the time of the packing qualification is the same as that at the time of operation.

Specific runs did show a marked increase in the variance over time, indicating that a change in the packed bed happened. An example of a change observed in the behavior of a particular packed bed is depicted in Fig. 9, where the RTD profiles are plotted for the initial pulse-input assessment along with the RTD profiles derived from six subsequent regeneration steps. Note that the first five profiles derived from the regeneration step are in very good agreement with the profile derived from the initial evaluation, but the sixth

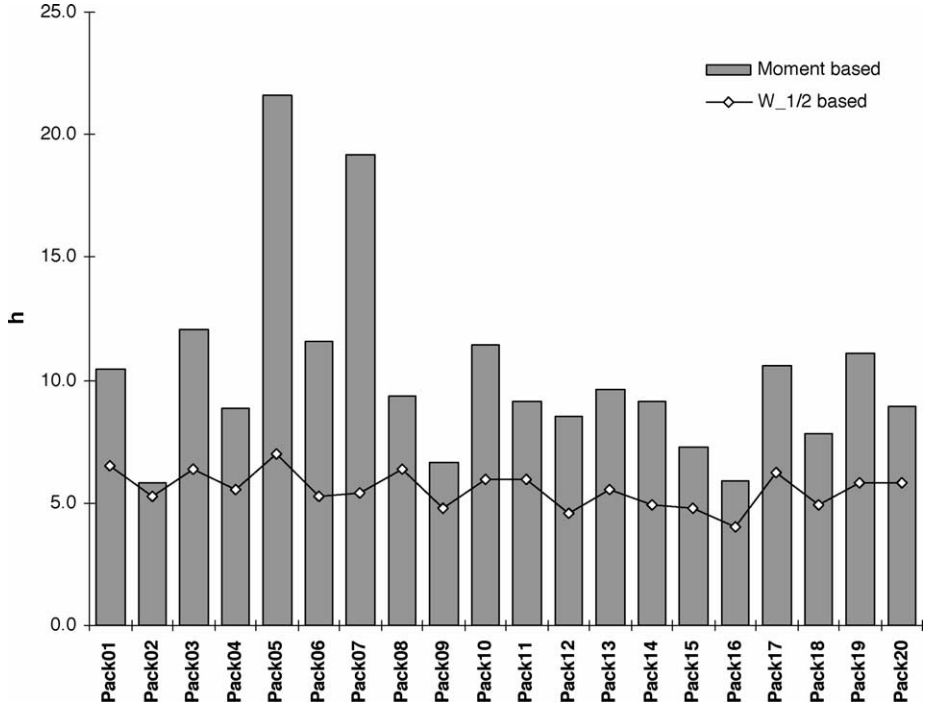

Fig. 6. Reduced plate height values for multiple packs of a representative process-scale chromatography column calculated from pulse-input RTDs (salt-based tracers). Plate heights were estimated using moments and from the $W_{1/2}$ values assuming a Gaussian peak.

regeneration profile shows an unusual double peak. This disagreement with the consistent preceding behavior indicates that a change in the packed bed occurred sometime after the fifth use of the column. This example further demonstrates the utility of RTD analysis for characterizing the consistency of the packed bed behavior. Agreement between the packing evaluation RTD and subsequent in-process RTDs provides assurance that the bed behavior at the time of the initial

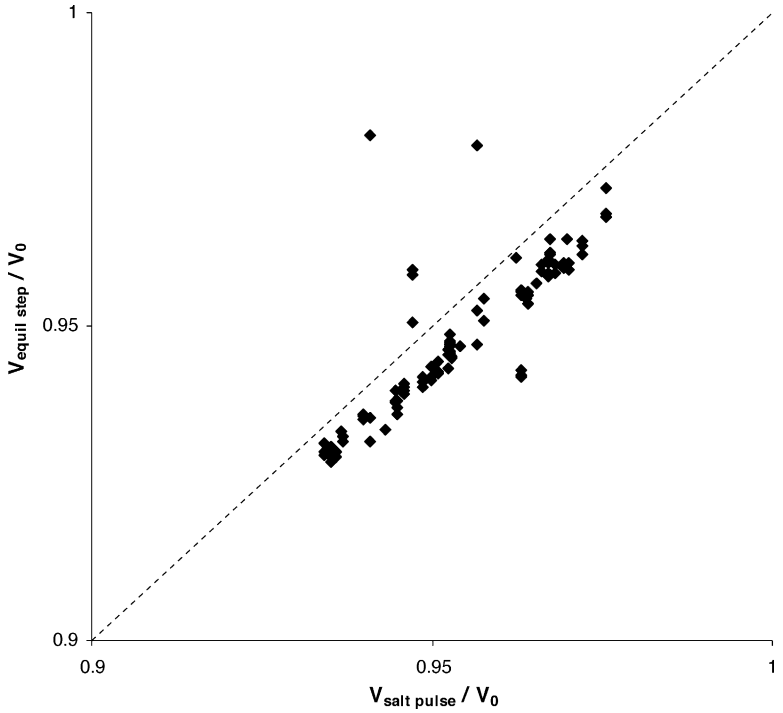

Fig. 7. The mean residence volumes calculated from conductivity transitions associated with a particular equilibration step ($V_{\text{equil step}}$) are plotted against the mean residence volumes calculated from the initial pulse-input for the same column ($V_{\text{salt pulse}}$).

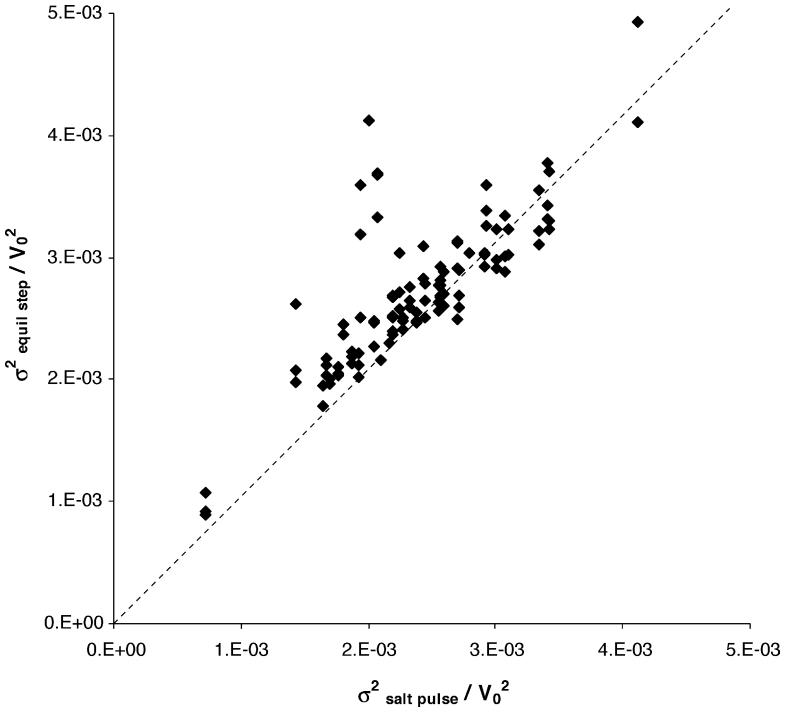

Fig. 8. The variances calculated from conductivity transitions associated with a particular equilibration step ($\sigma^2_{\text{equil step}}$) are plotted against the variances calculated from the initial pulse-input for the same column ($\sigma^2_{\text{salt pulse}}$).

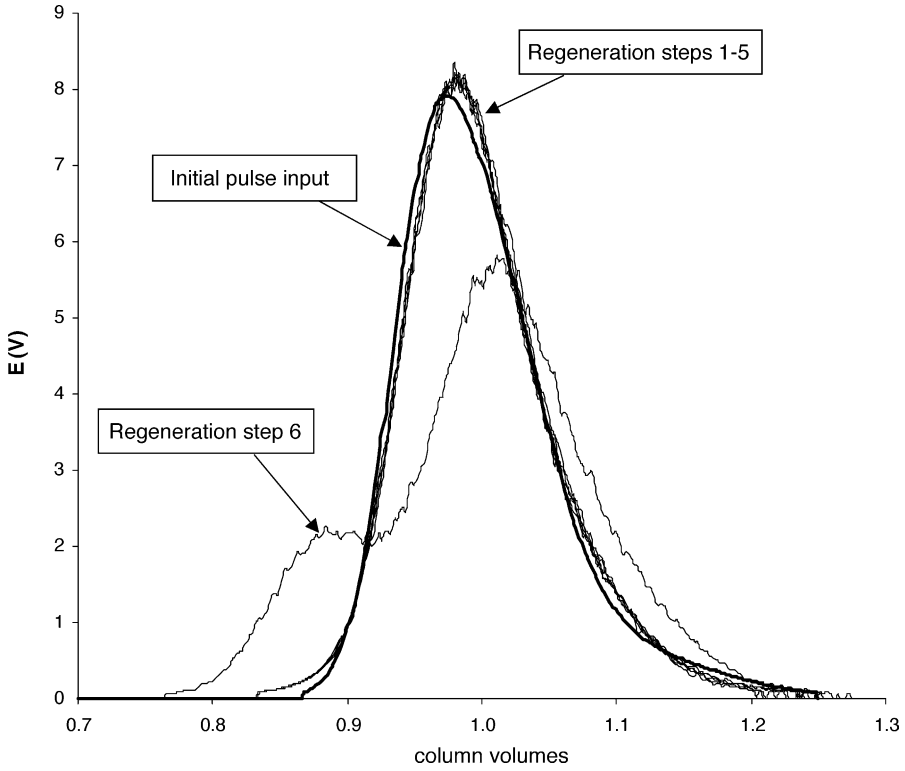

Fig. 9. RTD profiles obtained from the initial pulse-input evaluation and six subsequent conductivity transitions associated with a particular regeneration step (applying Eq. (3) to the step transitions).

qualification is the same as the behavior observed during subsequent operation. Moreover, any significant differences detected provide warning regarding potential problems.

3.3. Efficiency data and step performance

In addition to monitoring efficiency data from run to run, it is desirable to understand how these data relate to the performance of the chromatography step. Specifically, it is important to gain insight into the connection between the efficiency determined from experiments conducted with salt-based solutes, the efficiency expected for proteins and the outcome of protein separations.

It has been shown that the plate heights derived from experiments using small salt-based tracers are not representative of the plate heights expected for larger protein solutes [24]. It is expected that the plate heights for salt-based solutes should be primarily dominated by the macroscopic and axial dispersion resistances to mass transfer while protein-based plate heights should be governed mostly by the intraparticle diffusion resistance [22]. Smaller solutes have higher diffusivities, thus their transport by diffusion inside the particles is much faster. This expectation is confirmed by the van Deemter plot depicted in Fig. 10. This chart presents the data measured in this study for salt-based solutes along with estimates for two proteins of different size: interferon (MW, ca. 19 kDa) and immunoglobulin (MW, ca. 150 kDa). The parameters used to estimate the diffusional contributions for all solutes are presented in Table 2. As seen in Fig. 10, the overall reduced plate heights measured in this study for salt-based solutes at low values of the reduced velocity (ReSc) are much greater than the estimated contributions via Eqs. (14) and (15) for the diffusional resistances to mass transfer. Thus, the main contributions to band broadening for salt-based solutes come from the mass transfer resistances originated by axial and macroscopic dispersion.

Table 2
Parameters used to predict the reduced plate heights for the protein solutes in Fig. 10

Protein	v (cm/min)	D (cm^2/s)	d_p (μm)	ε_b	ε_p
Interferon	1.0	6.0×10^{-7}	90	0.35	0.88
IgG	1.0	4.0×10^{-7}	90	0.35	0.88

Diffusion coefficients were estimated following Tyn and Gusek [26]. The interstitial void fraction and intraparticle inclusion porosity were approximated using data from Nash and Chase [24].

On the other hand, it is also evident from Fig. 10 that the overall values of the reduced plate height for protein solutes are primarily determined by the contribution of intraparticle mass transfer resistance. As stated before, the overall values of the plate heights for the proteins were calculated by adding the estimated diffusional contributions (Eqs. (13) and (14)) to the axial and macroscopic dispersion contributions derived from the experiments with salt-based solutes (Eq. (15)). The calculated variability of the overall reduced

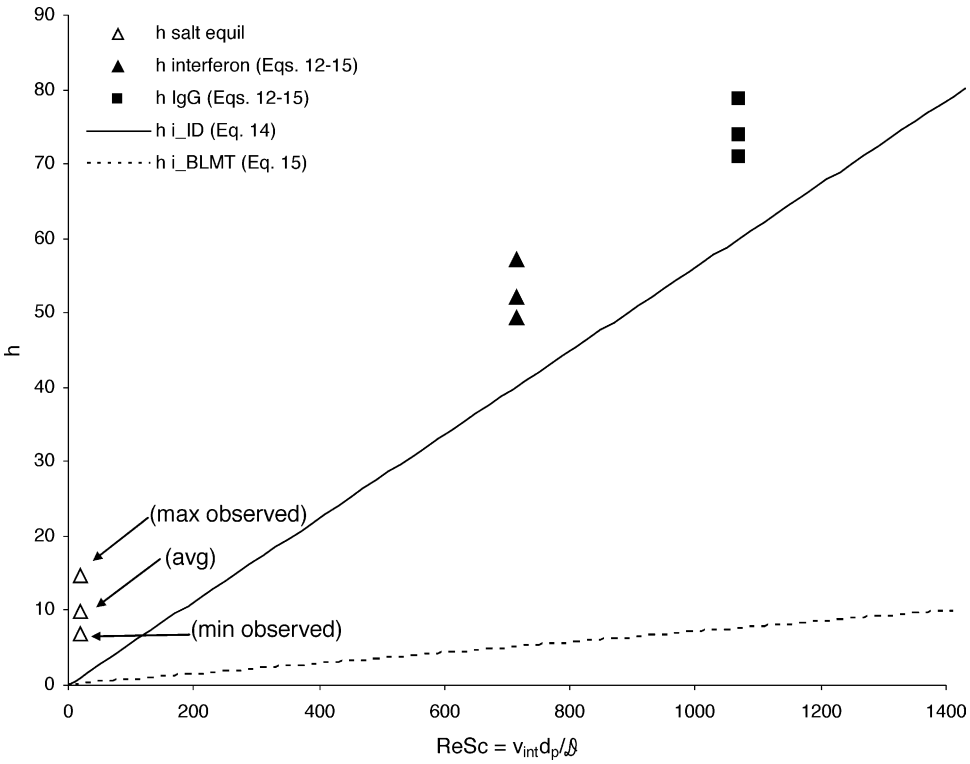

Fig. 10. Reduced plate heights versus reduced velocity for different solutes. The data for salt-based tracers were measured during equilibration or regeneration steps and the plate heights were estimated using moments. The data for the protein solutes were predicted using Eqs. (12)–(15). The smooth line and dotted line represent the predictions for boundary-layer mass transfer (Eq. (13)) and intraparticle diffusion (Eq. (14)), respectively.

plate height values for the proteins as a result of the run-to-run differences due to axial and macroscopic dispersion contributions is a fairly small fraction (ca. 10–20%) of the overall efficiency value. Thus, the observed run-to-run variations of the packing behavior should not have a major impact on the column efficiency during the actual separation of proteins.

Furthermore, note that the calculations presented in Fig. 10 are valid for conditions where the solutes are not retained. The plate height increases (and the efficiency decreases) as the protein retention increases [22]. During the course of a typical purification cycle, proteins are strongly retained during column load and weakly retained during column elution. Since the efficiency of the column increases as the separation progresses from the loading step to the elution step, the plate heights presented in Fig. 10 will be the smallest possible (and the efficiency the highest) to be encountered during the purification. The actual efficiency governing the separation of the proteins will be lower than the one expected from Fig. 10. Accordingly, the difference between the efficiency determined for a non-retained, salt-based solute and the efficiency expected for a retained protein is even bigger than the one depicted in Fig. 10.

If the separation of proteins is primarily governed by scale-independent contributions to mass transfer resistance due to intraparticle diffusion, it would be expected that the values of the plate heights determined for salt-based solutes should not exhibit a significant correlation with step performance. In fact, for different types of chromatography steps used in large-scale protein purification, we have observed the absence of a strong correlation between salt-based column efficiencies and step yield and purity (Proprietary data, not shown). Thus, the salt-based plate heights evaluated from the analysis of in-process step data are useful for characterizing the packing stability over time but might not be very useful for predicting the outcome of the step. If, however, a specific packing would originate an anomalous RTD profile for a salt-based solute (e.g. a wide split peak that could indicate the existence of channeling in the packed bed), it is possible that the value of the plate height for the salt-based solute under these circumstances can be of the same order of magnitude or higher than the value of the contribution to the plate height from the protein intraparticle diffusion. In this case it would be recommended to repack the column since the poor behavior of the packing could definitely affect the outcome of the protein separation.

4. Conclusions

RTD analysis of a conductivity-based pulse eluting from a freshly packed column is a useful tool for column evaluation and characterization. The first moment, or mean residence volume, provides a more accurate measure of the column hold-up volume than the value of the volume determined from the effluent peak maximum. The latter varies as a function of column dispersion, while the former is not dependent on column dispersion. The second central moment, or variance, is a very sensitive measure of the dispersion about the mean residence volume. The variance estimated via the second central moment includes most of the experimental RTD points in the calculation, effectively capturing tailing phenomena happening at the base of the peak.

Statistical moments can also be calculated from stepwise, in-process, conductivity-based transitions in order to characterize the packing behavior of process-scale chromatography columns at the actual time of use. These moments may be used to track the column behavior over multiple runs and to check for consistency with preceding runs and with the initial packing qualification. Significant changes in the behavior of the packed bed from run to run can be identified with this technique, thus aiding in the decision making process regarding the suitability of the column for future use. Thus, the RTD analysis of in-process step transitions could be a useful tool to be applied within the process analytical technology (PAT) framework recently proposed by the FDA [25]. As suggested by other authors [14,15] this tool could potentially provide timely evaluation of important process attributes such as the ability of the step to reduce the potential virus load of the feed.

Reduced plate heights were calculated from experiments with salt-based tracers in order to assess column efficiency under these conditions. Because the separation of interest typically involves proteins, plate height correlations were used to estimate the column efficiencies for protein solutes. Since the contribution of intraparticle diffusion to the overall plate height is the largest and most important factor that determines the column efficiency during the separation of proteins, it follows that random variations in the packing behavior as estimated from experiments conducted with salt-based tracers should not have a significant impact on the outcome of a protein separation (unless there is a significant breach of the integrity of the packed bed such as channeling). Therefore, monitoring the bed behavior using salt-based, stepwise, in-process conductivity transitions should be very useful for demonstrating control and consistency of the operation but of limited use as a way to determine the performance of a protein separation step.

5. Nomenclature

c	effluent conductivity (mS/cm)
d_p	diameter of a stationary-phase particle (cm)
D	mobile phase solute diffusion coefficient (cm^2/s)
$E(V)$	RTD function of an inert tracer
$F(V)$	age function of an inert tracer
h	reduced plate height
k_c	concentration-based fluid mass-transfer coefficient (cm/s)
L	column length (cm)

m	intraparticle diffusion resistance, given by $2.5/\varepsilon_p$
N	number of theoretical plates
Nu	fluid-phase Nusselt number, defined as $k_c d_p/D$
$ReSc$	reduced velocity, defined as $d_p v_{int}/D$
s	skewnees of the RTD
v_{int}	interstitial solute velocity (cm/s)
V	elution volume (L)
V_{mean}	mean residence volume (L)
V_o	bed volume (L)
V_{peak}	volume of effluent at the peak maximum (L)
x	fraction of solute in the mobile liquid phase, given by $\varepsilon_b/[\varepsilon_b + (1-\varepsilon_b)\varepsilon_p]$

Greek symbols

ε_b	interstitial (interparticle) void fraction in a packed bed
ε_p	intraparticle inclusion porosity of a solute
γ	third central moment of the RTD (L^3)
σ^2	variance of the RTD (L^2)

Acknowledgements

We thank John Bowers, Douglas Inloes, Andres Frei and Marcio Voloch for the useful technical discussions held during the execution of this work.

References

[1] G. Guiochon, S.A. Shirazi, A.M. Katti, Fundamentals of Preparative and Nonlinear Chromatography, Academic Press, New York, 1994.
[2] M.R. Ladisch, Bioseparations Engineering: Principles, Practice, and Economics, Wiley-Interscience, New York, 2001.
[3] S. Yamamoto, K. Nakanishi, R. Matsuno, Ion Exchange Chromatography of Proteins, Marcel Dekker, New York, 1988.
[4] J.C. Giddings, Unified Separation Science, Wiley, New York, 1991.
[5] J.H. Knox, J. Chromatogr. A 960 (2002) 7.
[6] M. Hofmann, J. Chromatogr. A 796 (1998) 75.
[7] J. Moscariello, G. Purdom, J. Coffman, T.W. Root, E.N. Lightfoot, J. Chromatogr. A 908 (2001) 131.
[8] A. Williams, K. Taylor, K. Dambuleff, O. Persson, R.M. Kennedy, J. Chromatogr. A 944 (2002) 69.
[9] M. Hofmann, J. Chromatogr. A 989 (2003) 79.
[10] T.M. Larson, J. Davis, H. Lam, J. Cacia, Biotechnol. Prog. 19 (2003) 485.
[11] E.A. Nack, B.L. Williamson, R.N. Keener, Presented at the 227th ACS National Meeting, Division of Biochemical Technology, Anaheim, CA, 2004.
[12] A.S. Rathore, R.M. Kennedy, J.K. O'Donnell, I. Bemberis, O. Kaltenbrunner, BioPharm 3 (2003) 30.
[13] A. Sonnenfeld, H. Forrester, J. Thommes, Presented at the 227th ACS National Meeting, Division of Biochemical Technology, Anaheim, CA, 2004.
[14] K. Brorson, Presented at the 227th ACS National Meeting: Division of Biochemical Technology, Anaheim, CA, 2004.
[15] L. Norling, S. Lute, R. Emery, Y. Xu, Q. Chen, G. Blank, K. Brorson, Presented at the 17th International Symposium on Preparative/Process Chromatography, Baltimore, MD, 2004.
[16] E.N. Lightfoot, J.L. Coffman, F. Lode, Q.S. Yuan, T.W. Perkins, T.W. Root, J. Chromatogr. A 760 (1997) 139.
[17] E.N. Lightfoot, J.S. Moscariello, M.A. Teeters, T.W. Root, in: A.S. Rathore, A. Velayudhan (Eds.), Scale-Up and Optimization in Preparative Chromatography: Principles and Biopharmaceutical Applications, Marcel Dekker, New York, 2003, p. 33.
[18] B.A. Bidlingmeyer, F.V. Warren, Anal. Chem. 56 (1984) 1583A.
[19] R.H. Perry, D.W. Green (Eds.), Perry's Chemical Engineer's Handbook, second ed., McGraw-Hill, New York, NY, 1997, pp. 3–53.
[20] R.G. Carbonell, B.J. McCoy, Chem. Eng. J. 9 (1975) 115.
[21] A.M. Athalye, S.J. Gibbs, E.N. Lightfoot, J. Chromatogr. 589 (1992) 71.
[22] V. Natarajan, S. Cramer, Sep. Sci. Technol. 35 (2000) 1719.
[23] M.A. Teeters, T.W. Root, E.N. Lightfoot, J. Chromatogr. A 944 (2001) 129.
[24] D.C. Nash, H.A. Chase, J. Chromatogr. A 807 (1998) 185.
[25] US Food and Drug Administration (FDA), Draft Guidance for Industry: PAT—A Framework for Innovative Pharmaceutical Manufacturing and Quality Assurance, Rockville, MD, 2004.
[26] M.T. Tyn, T.W. Gusek, Biotechnol. Bioeng. 35 (1990) 327.